applied sciences

MDPI

Article

The Design and Simulation of an Astronomical Clock

Branislav Popkonstantinović [1,*], Ratko Obradović [2], Miša Stojićević [1], Zorana Jeli [1], Ivana Cvetković [1], Ivana Vasiljević [2] and Zoran Milojević [3,*]

[1] Faculty of Mechanical Engineering, University of Belgrade, 11000 Belgrade, Serbia; mstojicevic@mas.bg.ac.rs (M.S.); zjeli@mas.bg.ac.rs (Z.J.); icvetkovic@mas.bg.ac.rs (I.C.)
[2] Faculty of Technical Sciences, University of Novi Sad, 21000 Novi Sad, Serbia; obrad_r@uns.ac.rs (R.O.); ivanav@uns.ac.rs (I.V.)
[3] School of Engineering, Newcastle University, Newcastle upon Tyne NE1 7RU, UK
* Correspondence: bpopkon@mas.bg.ac.rs (B.P.); Zoran.Milojevic@newcastle.ac.uk (Z.M.)

Abstract: This paper describes and explains the synthesis of an astronomical clock mechanism which displays the mean position of the Sun, the Moon, the lunar node and zodiac circle as well as the Moon phases and their motion during the year as seen from the Earth. The clock face represents the stereographic projection of the celestial equator, celestial tropics, zodiac circle (ecliptic) and horizon for the latitude of Belgrade from the north celestial pole to the equator plane. The observed motions of celestial objects are realized by a set of clock gear trains with properly calculated gear ratios. The method of continued fraction is applied in the computation of proper and practically applicable gear ratios of the clock gear trains. The fully operational 3D model of the astronomical clock is created and the motion study of its operation is accomplished by using the SolidWorks 2016 application. The simulation results are compared with the ephemeris data and the detected differences are used to evaluate the long-term accuracy of the astronomical clock operation. The presented methods of the clock mechanism synthesis can be useful for the design, maintenance and conservation of large-scale city astronomical clocks since these clocks represent a precious historical and cultural heritage of European civilization.

Keywords: astronomical clock; CAD; continued fractions; mechanisms; motion study; stereographic projection

Citation: Popkonstantinović, B.; Obradović, R.; Stojićević, M.; Jeli, Z.; Cvetković, I.; Vasiljević, I.; Milojević, Z. The Design and Simulation of an Astronomical Clock. *Appl. Sci.* **2021**, *11*, 3989. https://doi.org/10.3390/app11093989

Academic Editor: John Clayton

Received: 27 March 2021
Accepted: 20 April 2021
Published: 28 April 2021

1. Introduction

This paper describes the synthesis of an astronomical clock mechanism and explains the design of its dial. This astronomical clock determines and displays the mean positions of the Sun, the Moon, the lunar nodes and the zodiac circle as well as their motion during the year as seen from the Earth. Moreover, its mechanism calculates the phases of the Moon and demonstrates the evolution of its shape on an additional screen. The content of this work is divided into several sections. After short historical considerations of the design of some significant astronomical clocks which were installed in European cities during past centuries, the features of the modeled astronomical clock are presented. The next section explains the geometrical and astronomical characteristics of the astronomical clock face. It is disclosed and visually demonstrated that its design is based on stereographic projection of the celestial sphere. Astronomical data important for the design of the astronomical clock mechanism and approximations of their ratios by the method of continued fractions are presented in the succeeding sections. This is followed by the explanation of the modeling of the clock gear trains and the assembly synthesis of the complete clock mechanism. The next section gives insight into a process of determining the initial positions of the clock pointers for the correct simulation and the motion study of the clock mechanism operation. In the following section, the numerical data obtained by the simulation are tabulated, analyzed and compared with the astronomical ephemeris data. In the penultimate section,

the detected differences are used to inspect, evaluate and discuss the long-term accuracy of astronomical clock operation. Furthermore, in the same section, the design of the presented clock is compared with the famous Prague astronomical clock and it is disclosed that the Prague clock is less accurate. Finally, in the last section, the importance of this paper is briefly indicated. It is emphasized that the main contribution of this work lies in disseminating and protecting knowledge, the loss of which risks making these precious clocks no longer restorable.

2. Historical Background

Astronomical clocks appeared in Europe as a reflection of the cultural and scientific revival during the period of the Renaissance. One of the earliest known astronomical clocks is Le Gros Horloge in Rouen [1], shown in Figure 1, probably one of the oldest in France whose movement was made in 1389. The mechanism of this astronomical clock is very large but quite simple. It displays only the daily motion of the Sun and lunar phases.

Figure 1. Le Gros Horloge in Rouen, France [2].

The Strasbourg astronomical clock [1], in Figure 2, installed in the Cathédrale Notre-Dame of Strasbourg in the 17th century, is the third in this location. The first clock had been built in the 14th century and the second one in the 16th century. The current clock, displayed in Figure 2, computes and demonstrates many astronomical data including the correct dates of Easter.

The most famous astronomical clock in Europe is the Old Town Hall clock in Prague, also known as the Prague Orloj [1], constructed in 1410. Its most recognizable characteristic, clearly visible in Figure 3, is the dial designed as a stereographic projection of the celestial sphere.

Figure 2. The Strasbourg astronomical clock [3].

Figure 3. Prague Orloj, Czech Republic [4].

Interesting enough to be mentioned is another horologium in the Czech Republic, the one in the city of Olomouc [1]. It is a rare example of a heliocentric astronomical clock. Contrary to the fact that the vast majority of astronomical clocks were built in past centuries, there are some examples of modern clocks of this type. One of the recently

constructed astronomical clocks, shown in Figure 4, installed in 2009 in the municipality of Stará Bystrica [1], is the only astronomical clock in Slovakia. Similarly to the face of Prague Orloj, its display consists of an astrolabe but, unlike Prague Orloj, its mechanism is controlled by a computer using a German longwave time signal.

Figure 4. The clock of Stará Bystrica, Czech Republic [5].

Astronomical clocks were important horological and astronomical instruments in past centuries. Today, they represent the precious historical and cultural heritage of European civilization. That is the main reason why the art of the astronomical clock design and the skills for the maintenance and conservation of their mechanisms should not be forgotten.

3. Features of the Modeled Astronomical Clock

The astronomical clock whose design and motion study are presented in this paper will be capable of determining the mean positions of the Sun, the Moon, the lunar nodes and the zodiac circle as well as their motions during the year as seen from the Earth. This means that the locations and movements of the previously mentioned celestial objects are displayed on the astronomical clock face which represents the stereographic projection of the celestial sphere from the north celestial pole to the equator plane. In particular, the clock face indicates the celestial equator, meridian of a place, celestial tropics (Tropic of Cancer and Tropic of Capricorn), zodiac circle (ecliptic) and the horizon and set of almucantars above the horizon, as well as the almucantars of civil, nautical and astronomical twilights for the latitude of Belgrade. Moreover, the clock mechanism determines the phases of the Moon and displays them on an additional and separate screen.

Since the modeled astronomical clock indicates simultaneously the mean positions of the Sun, the Moon and the zodiac circle during the year, the following data can be observed straightaway on its dial: local mean solar time, local mean sidereal time, the position of the Sun and the Moon on the ecliptic plane (in zodiac circle), the angular distance between the Moon and the Sun which determines the phase of the Moon, the altitude of the Sun and the local time of sunset, sunrise, dusk and dawn. The date of the winter and summer solstices, as well as the date of vernal and autumnal equinoxes, can also be detected and shown on the clock dial. Besides this, the date of lunar and solar eclipses can also be predicted and determined sufficiently accurately because the clock mechanism indicates the position of the lunar nodes.

4. The Face of the Astronomical Clock

The positions of the celestial objects on the celestial sphere are determined by angular coordinates (altitude—azimuth, declination—right ascension or ecliptic latitude and longitude). Since the stereographic projection is conformal and thus preserves angles, it can

be used for the design of the astronomical dial. The construction of the astronomical dial for the latitude of Belgrade (44.80 N) will be presented and explained in this paper in all necessary detail.

Since the celestial sphere rotates around the celestial axis *NS*, the dial of this astronomical clock can be geometrically constructed by the stereographic projection of characteristic circles on the celestial sphere from the celestial pole *N* or *S* to the plane of the celestial equator *e*. Since Belgrade is located in the northern hemisphere, the stereographic projection is obtained from the North Pole *N*. As is shown on Figure 5, the zodiac circle (circle of ecliptic) *z*, the celestial Tropic of Capricorn t_S, the celestial Tropic of Cancer t_N and the horizon *h* for the latitude of Belgrade are stereographically projected from the pole *N* to the plane of the celestial equator *e*. The circles of ecliptic *z* and celestial equator *e* intersect at two points: one of them is the first point of Aries or the cusp of Aries γ and the second one is the first point of Libra Ω. As usual, the astronomical dial is rimmed by the celestial Tropic of Cancer t_N since the Sun and the Moon, as observed from the Earth, never exceed this circle. The zodiac circle (the circle of ecliptic) *z* just touches both celestial tropics and intersects equator *e* and horizon h at the same pair of points—γ and Ω.

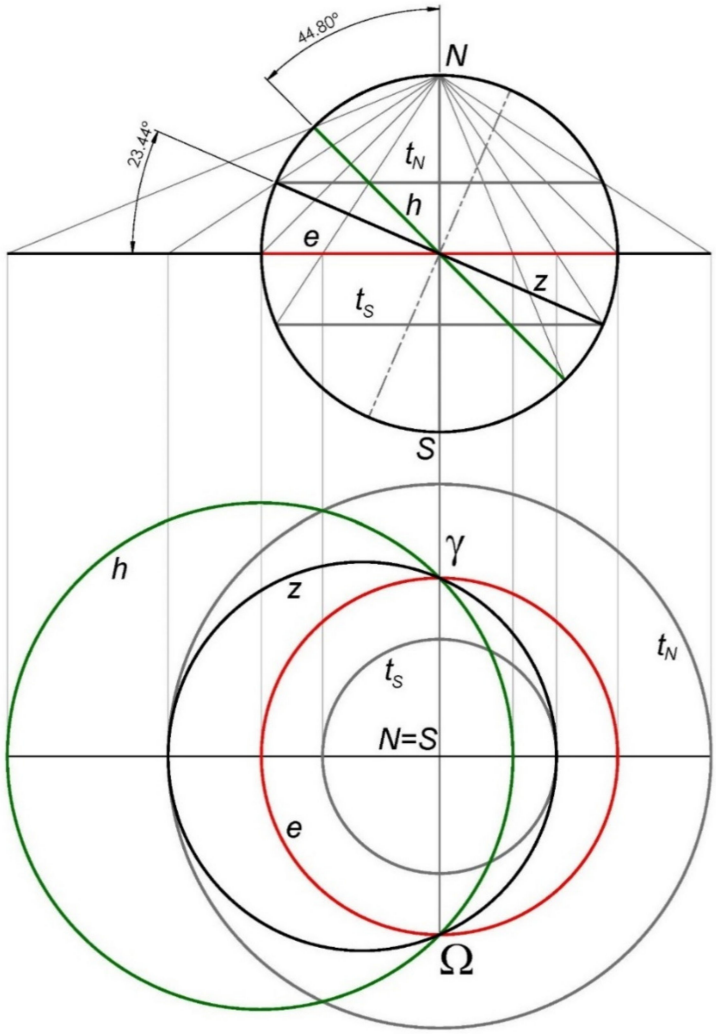

Figure 5. The stereographic projection of the celestial sphere.

Due to the fact that the positions of the Sun and the Moon are determined on this astronomical dial by the ecliptic longitude, the representation of the ecliptic circle (zodiac) is a crucial and inevitable part of its face. Thus, the zodiac circle must be geometrically constructed as well. The stereographic projections of the zodiac circle and its division into

12 equal segments from the pole *N* to the plane of the celestial equator are given in Figure 6. The zodiac circle is stereographically divided into 12 equal segments each of which is 30 degrees of ecliptic longitude wide. These segments are named after the well-known astrological signs: Aries P, Taurus Q, Gemini R, Cancer S, Leo T, Virgo U, Libra V, Scorpio W, Sagittarius X, Capricorn ♑, Aquarius ♒, and Pisces a. All segments are equally graduated with six divisions of five degrees each. It is important to emphasize what can be easily seen on the zodiac circle, namely that stereographic projections of these divisions are unevenly distributed since the stereographic projection is not affine but central.

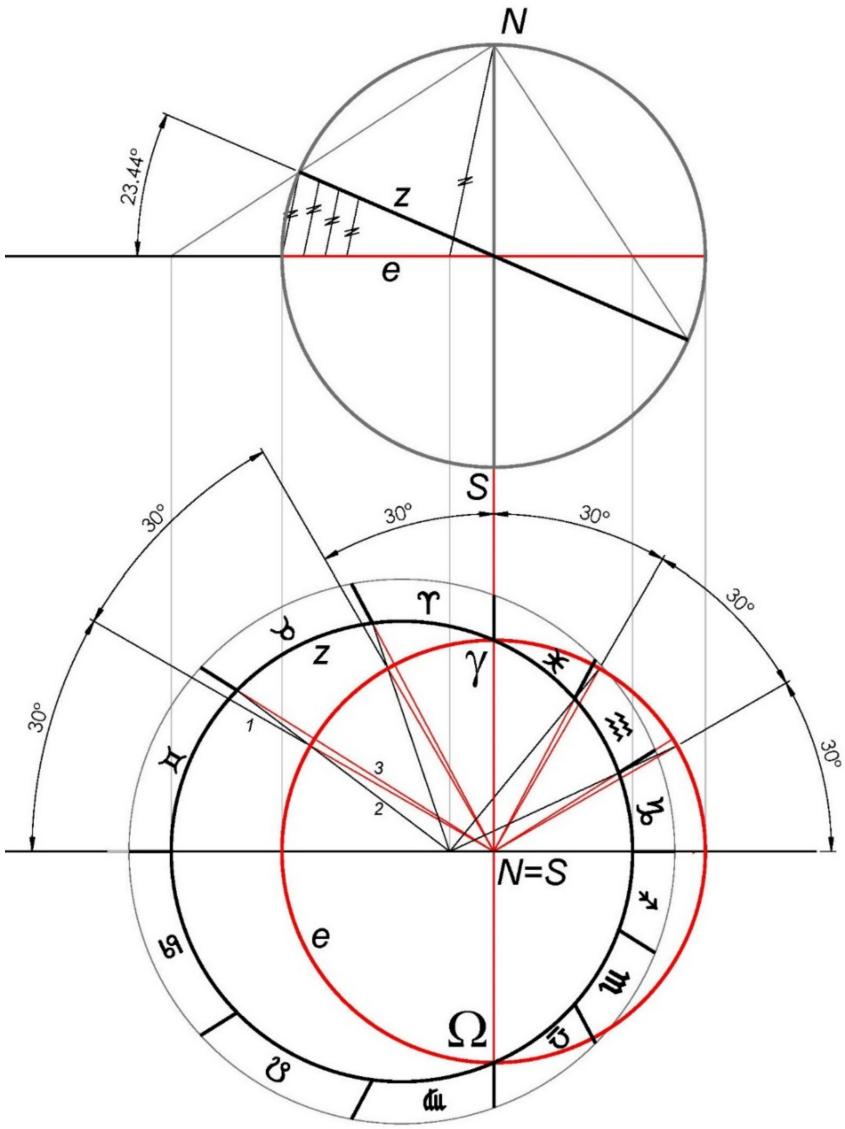

Figure 6. The stereographic projection of the zodiac and its division into 12 equal segments.

Figure 7 shows the model of an astronomical dial created by the SolidWorks application. The Sun (4) and the Moon (16) symbols (icons) are attached to the clock hands which rotate around the clock axis (13). The zodiac (ecliptic) circle (14) also rotates around the axis (13) and supports the Sun and the Moon icons by the two circular grooves. By the position of the Sun pointer, the local mean solar time can be read on the 24 numeral divisions placed at the edge of the celestial Tropic of Cancer (3). By the position of the arrow mark (2) (γ) at the zodiac (14), the local mean sidereal time can also be determined on the same division (3) or on the equator circle (8) scale. The ring (12) is the celestial Tropic of Capricorn and represents the inner border of the dial. The position of the Sun (4) on the ecliptic circle (14)

indicates the current date of the year. The apparent angular distance between the Sun (4) and the Moon (16) hands determines the Moon phase. This angular distance can be read out directly in days on the tiny ring (17) attached to the Sun pointer. The Moon phases can also be seen in a more pictorial and vivid way on a separate display equipped with rotational sphere (9) which is painted half white and half dark blue. The astronomical dial has the projection of the local horizon (6) and five almucantars (5) at the angular distance of 12°. The daytime period (1) and the astronomical night (10) are indicated by the position of the Sun icon above and below the horizon, respectively.

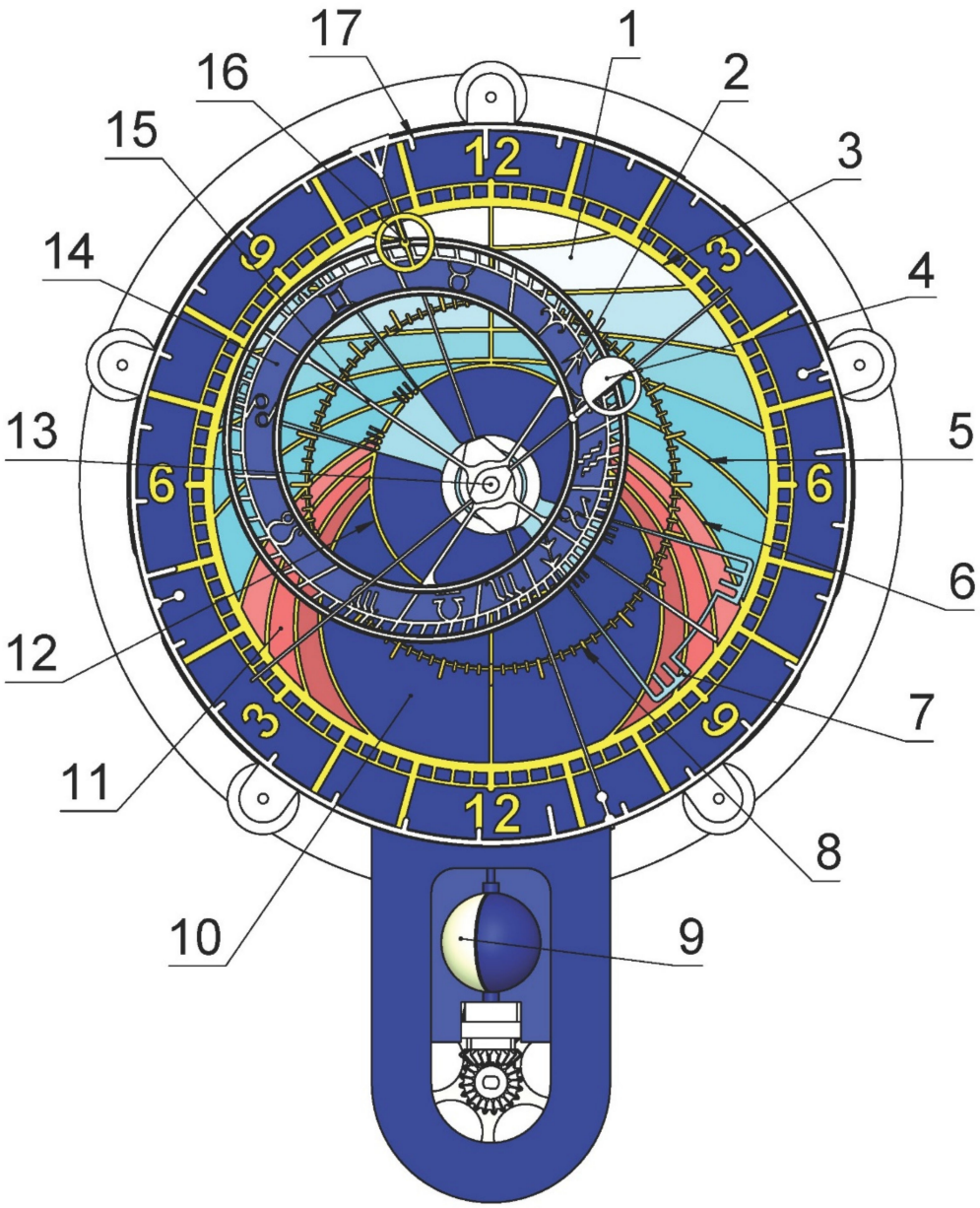

Figure 7. The model of the astronomical dial.

The altitude of the Sun can be determined approximately correctly (with an error of ±3°) by the aforementioned almucantars. The Sun icon positioned on the horizon determines the time of sunrise or sunset. Three almucantars (11) are also displayed below the horizon, at the angular distance of 6°, illustrating the periods of civil, nautical and astronomical twilights (11). The interval between sunset and dusk is determined on the right side of the dial, while the interval between dawn and sunrise is on its left side. The astronomical dial is equipped with a lunar node pointer (15) and corresponding circular

sectors (7) which play an important role in the prediction of lunar and solar eclipses. The meaning of these sectors will be explained in the next section dedicated to the astronomical data necessary for the proper construction of the astronomical clock mechanism.

5. The Astronomical Data

It is evident that all the intended features of the astronomical clock disclosed and explained in Section 3 can be obtained not just by the proper construction of the dial, but also by the correct design of the clock mechanism. The synthesis of the astronomical clock mechanism is based on certain well-known astronomical facts and numerical data. The ratio between these data will be interpreted and realized by the clock mechanism gear ratios. Therefore, all astronomical data which are necessary for the design of the clock mechanism must be carefully considered and properly selected.

First, the Earth rotates around its axis which is currently tilted 23.444 degrees from its orbital axis [6]. From the viewpoint on the Earth, the Sun rotates from the east to the west with the period known as a solar day with a mean length of 24 h. The apparent path of the Sun during the year, as seen from the Earth, passes through the zodiac which is divided into 12 signs and form the ecliptic coordinate system. The Sun's position at the vernal equinox is the origin of ecliptic longitude. From an observer on the Earth, the zodiac rotates daily to the west within the period known as sidereal day whose mean length, determined for the year 2019, is 23 h 56 min 4.09053 s or 23.934469592 h [7].

The period of the Moon's orbit with respect to the line which connects the Earth and the Sun, or the period of lunar phases, is called a synodic month. This period varies over time but its mean value calculated for a long period of time is extremely stable. Currently, the average duration of the synodic month is T_{Ph} = 29.530589 days [6,8] and is decreasing in mean length by about 3.6×10^{-7} solar days per century [6] or by about 0.311 s per millennium.

Since the astronomical clock displays the daily motion of the Moon, the average period of the Earth's rotation relative to the Moon, or tidal lunar day, must be calculated. From the fact that the angular distance between the Sun and the Moon determines the lunar phase, the mean value of the tidal lunar day can be determined from Equation (1):

$$T_L = 24\left(\frac{1}{T_S} - \frac{1}{T_{Ph}}\right)^{-1} = 24\left(1 - \frac{1}{29.530588}\right)^{-1} = 24.8412024 \text{ h} \quad (1)$$

The orbit of the Moon is inclined to the ecliptic and crosses the ecliptic in two lunar nodes: the ascending node and the descending node [9]. The lunar nodes revolve slowly around the ecliptic [9] in the direction opposite to the direction of the Earth's revolution. The period of the lunar node cycle determined for the year 2019 is T_N = 18.612952 years [8]. The mean interval of time between two successive conjunctions of the Sun with the same lunar node is called the eclipse year and lasts T_E = 346.620067 days [8]. It is a little bit shorter than the solar year because the directions of nodal precession and the Earth's revolution are opposite. The lunar nodes play an important role in the explanation of the phenomena called lunar and solar eclipses. From the viewpoint of an observer on the Earth, a solar eclipse can occur only when the Moon and the Sun are both near the same node, and a lunar eclipse can only happen when the Sun and the Moon are close to opposite lunar nodes. If the angle between the line of nodes and the Moon or the Sun is less than 9°30′, a lunar eclipse must occur, while if it is greater than 12°15′, a lunar eclipse is not possible (lunar eclipse limit). If the abovementioned angle is less than 15°23′, a solar eclipse must happen, while if it is more than 18°35′, a solar eclipse cannot occur (solar eclipse limit) [10].

All the astronomical data important for the synthesis of the astronomical clock mechanism are given in Table 1.

Table 1. The astronomical data.

Astronomical Data	Duration	Astronomical Data	Duration
Solar day	$T_S = 24$ h	Lunar tidal day	$T_L = 24.8412024$ h
Sidereal day	$T_{SID} = 23.934469592$ h	Lunar nodal period	$T_N = 18.612952$ years
Synodic month	$T_{Ph} = 29.530588$ days	Eclipse year	$T_E = 346.620067$ days

6. Approximations of Astronomical Data

It is important to emphasize that the astronomical clock whose design is presented in this work determines and displays geocentrically not the apparent or true position but the mean position of the Sun, the Moon, the lunar nodes the zodiac circle and their motion during the year. All irregularities of the Sun, the Moon and the lunar node celestial motions are neglected for this mechanical model. In other words, it is presumed that the observed movements of the aforementioned objects across the celestial sphere are circular and uniform. These uniform circular motions are realized by a set of clock gear trains with meticulously calculated gear ratios.

Since the number of gear teeth is an integer, the gear ratios must be approximated by rational numbers. The proper gear ratios of the mechanism gear trains are determined by the method of continued fractions since this calculation technique was mathematically proven [11] to produce the best possible rational approximation of a real number [12]. (Given a number x, its best rational approximations of the first kind are those fractions p/q such that x is closer to p/q than to any fraction with a smaller denominator. Given a number x, its best rational approximations of the second kind are those fractions p/q such that for any fraction p'/q' with $q' < p$, we have $|q'x - p'| > |qx - p|$.) However, for this objective, the method of continued fractions is not sufficient. Since the diameter of the gear cannot be arbitrarily large nor can the gear modulus be arbitrarily small, the number of gear teeth is always limited by the clock dimensions and by the method of gear production. Thus, it is necessary to introduce an additional criterion which will determine the practically acceptable rational approximation obtained by the method of continued fractions. Basically, this precaution can be formulated as the limitation of the number of gear teeth and depends on gear production technology, gear modulus and dimensions of the clock. In this case, we are planning to produce gears by ABS filament 3D printing and since the clock face diameter is approximately 400 mm, the gear diameter should not be greater than 150 mm and the modulus not less than 1 mm.

Briefly, the previous considerations can be summarized as follows:

- The proper gear ratio of the particular gear train must be determined by the method of continued fractions. This method generates the set of convergents or semi-convergents of the continued fraction representation of the real ratio [12,13].
- The error of the chosen rational approximation should be sufficiently small.
- The rational approximation should be selected in such a way that prime factors of their numerators and denominators are less than 150.

The operational scheme of the astronomical clock mechanism, which consists of a set of gear trains, is given in Figure 8. In this figure, *C* is the input hour shaft of the ordinary clock, *S* is the Sun, *M* is the Moon, *Z* is the zodiac, *Ph* is the lunar phases and *N* represents lunar nodes. In the same figure, $R_{CS} = 2:1$ is the ratio between angular velocities of the clock hour shaft and the astronomical clock's Sun pointer. R_{SM} is the ratio between angular velocities of the Sun and the Moon pointers, R_{MZ} is the Moon and the zodiac, R_{SPh} is the Sun and the lunar phases and R_{SN} is the ratio between angular velocities of the Sun and the lunar node pointers on the same astronomical dial. These ratios are approximated by the set of continued fractions convergents *(C)* and semi-convergents *(SC)* and the prime factors of their numerators and denominators are determined. To demonstrate these calculations more concisely, not all convergents and semi-convergents are presented, but only the range from the first to the one which is accepted as a sufficiently correct approximation. The set of best rational approximations of the ratio R_{SPh} =29.530589 is given in Table 2.

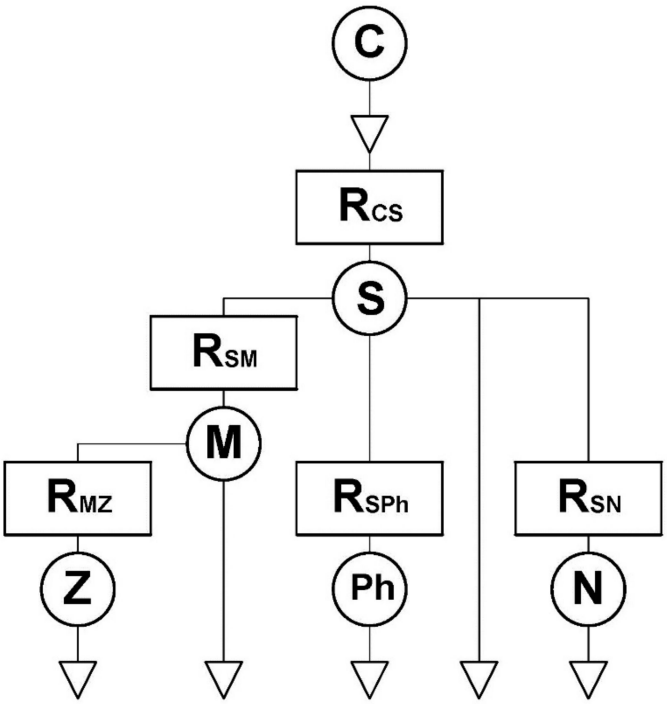

Figure 8. The operational scheme of the astronomical clock mechanism.

Table 2. The best rational approximations of the ratio R_{SPh}.

Type	Approximation	Type	Approximation
C	$29/1$	SC	$384/13 = 2^7 \times 3/13$
C	$30/1 = (2 \times 3 \times 5)/1$	C	$443/15 = 443/(3 \times 5)$
C	$59/2$	C	$502/17 = 2 \times 251/17$
SC	$266/9 = 2 \times 7 \times 19/3^2$	SC	$945/32 = (3^3 \times 5 \times 7)/2^5$
SC	$325/11 = (5^2 \times 13)/11$	C	$1447/49 = 1447/7^2$

The semi-convergent 945/32 is chosen to approximate the ratio $R_{SPh} = 29.530589$. The error of this approximation is 0.000662 days per lunation or less than 12 min per year.

The ratio R_{SM} between angular velocities of the Sun and the Moon clock pointers is determined by Equation (2):

$$R_{SM} = \frac{T_L}{T_S} = \frac{24.8412024}{24} = 1.0350501 \quad (2)$$

The set of best rational approximations of the ratio R_{SM} is given in Table 3.

The semi-convergent 945/913 is selected as the approximation of the ratio R_{SM}. The absolute value of the error of this approximation is calculated from the following expression (3):

$$\left| 24 \times \frac{945}{913} - 24.8412024 \right| = 1.949 \times 10^{-5} \text{ h} \approx 0.07 \text{ s} \quad (3)$$

This error denotes that the mean position of the Moon will be determined by the clock mechanism with an error of approximately 0.07 s per day or less than 30 s per year.

Regarding the operational scheme of the astronomical clock mechanism given in Figure 8, the ratio R_{MZ} between the angular velocities of the Moon and the zodiac pointers is calculated by the following expression (4):

$$R_{MZ} = \frac{T_{SID}}{T_S} \times {R_{SM}}^{-1} = \frac{23.934469592}{24} \times \frac{913}{945} = 0.963499592 \quad (4)$$

Table 3. The best rational approximations of the ratio R_{SM}.

Type	Approximation	Type	Approximation
C	$1/1$	C	$30/29 = (2 \times 3 \times 5)/(2^2 \times 7)$
SC	$16/15 = 2^4/(3 \times 5)$	C	$59/57 = 59/(3 \times 19)$
SC	$17/16 = 17/2^4$	SC	$266/257 = (2 \times 7 \times 19)/257$
SC	$18/17 = (2 \times 3^2)/17$	SC	$325/314 = (5^2 \times 13)/(2 \times 157)$
SC	... ...	SC	$384/371 = (2^7 \times 3)/(7 \times 53)$
SC	$27/26 = 3^3/(2 \times 13)$	C	$443/428 = 443/(2^2 \times 107)$
SC	$28/27 = (2^2 \times 7)/3^3$	C	$502/485 = (2 \times 251)/(5 \times 97)$
C	$29/28 = 29/(2^2 \times 7)$	SC	$945/913 = (3^3 \times 5 \times 7)/(11 \times 83)$

The set of convergents (C) and semi-convergents (SC) by which the ratio R_{MZ} is approximately determined is given in Table 4. The convergent $26,001/26,986$ is selected as the approximation of the ratio R_{MZ}. Since the ratio between this convergent and the semi-convergent $913/945$ produces the rational approximation $\overline{T}_{SID}$ of the sidereal day by the following expression (5),

$$\overline{T}_{SID} = 24 \times \frac{26,001/26,986}{913/945} = 23.93446961 \text{ h}, \quad (5)$$

the absolute value of the error obtained by this approximation can be calculated from the expression (6)

$$\left|\overline{T}_{SID} - 23.934469592\right| = 2 \times 10^{-8} \text{ h} = 7.2 \times 10^{-5} \text{ s} \quad (6)$$

This value means that the clock mechanism determines the mean sidereal day with an error of approximately 7.2×10^{-5} s per day or less than 0.03 s per year.

Table 4. The best rational approximations of the ratio R_{MZ}.

Type	Approximation	Type	Approximation
C	$0/1$	SC	$1003/1041 = (17 \times 59)/(3 \times 347)$
C	$1/1$	SC	$1135/1178 = (5 \times 227)/(2 \times 19 \times 31)$
SC	$13/14 = 13/(2 \times 7)$	SC	$1267/1315 = (7 \times 181)/(5 \times 263)$
SC	$14/15 = (2 \times 7)/(3 \times 5)$	SC	$1399/1452 = 1399/(2^2 \times 3 \times 11^2)$
SC	... ...	SC	$1531/1589 = 1531/(7 \times 227)$
SC	$24/25 = 2^3 \times 3/5^2$	C	$1663/1729 = 1663/(7 \times 13 \times 19)$
SC	$25/26 = 5^2/(2 \times 13)$	C	$1795/1863 = (5 \times 359)/(3^4 \times 23)$
C	$26/27 = (2 \times 13)/3^2$	C	$3458/3589 = (2 \times 7 \times 13 \times 19)/(37 \times 97)$
C	$53/55 = 53/(5 \times 11)$	SC	$15,627/16,219 = (3 \times 5209)/(7^2 \times 331)$
C	$79/82 = 79/(2 \times 41)$	SC	$19,085/19808,808 = (5 \times 11 \times 347)/(2^5 \times 619)$
C	$132/137 = (2^2 \times 3 \times 11)/137$	SC	$22,543/23,395 = 22,543/(5 \times 4679)$
SC	$871/904 = (13 \times 67)/(2^3 \times 113)$	C	$26,001/26,986 = (3^5 \times 107)/(2 \times 103 \times 131)$

In accordance with the operational scheme of the clock mechanism, astronomical data given in Table 1 and the fact that the lunar nodal cycle is k = 18.612952 times longer than a year, the ratio R_{SN} between angular velocities of the Sun and the lunar node pointers can be determined by the following expression (Equation (7)):

$$R_{SN} = \left[\frac{T_S}{T_{SID}} + \left(\frac{T_S - T_{SID}}{T_{SID}}\right) \times \frac{1}{k}\right]^{-1} = 0.997123293 \quad (7)$$

The best rational approximations of the ratio $R_{SN} = 0.997123293$ are given in Table 5. The convergent $2773/2781$ is chosen as the best applicable approximation of the ratio R_{SN}. Since the difference between angular velocities of the Sun and the lunar node pointers represents the approximation of the lunar node angular velocity relative to the Sun, the next Equation (8) determines the approximation of the eclipse year $\overline{T}_E$.

$$\overline{T}_E = \left(\frac{2781}{1773} - T_S\right)^{-1} = \left(\frac{2781}{1773} - 1\right)^{-1} = 346.6250162 \text{ days} \quad (8)$$

Thus, the mechanism of the astronomical clock approximates the eclipse year with an error whose absolute value is determined by the following expression (9):

$$\left|\overline{T}_E - T_E\right| = |346.6250162 - 346.620067\,| = 0.0049492 \text{ days} \approx 7.13 \text{ min} \quad (9)$$

Table 5. The best rational approximations of the ratio R_{SN}.

Type	Approximation	Type	Approximation
C	$0/1$	C	$346/347 = (2 \times 173)/347$
C	$1/1$	C	$347/348 = 347/(2^2 \times 3 \times 29)$
SC	$173/174 = 173/(2 \times 3 \times 29)$	C	$693/695 = (3^2 \times 7 \times 11)/(5 \times 139)$
SC	$174/175$	C	$1040/1043 = (2^4 \times 5 \times 13)/(7 \times 149)$
SC	... ...	C	$1733/1738 = 1733/(2 \times 11 \times 79)$
SC	$345/346 = (3 \times 5 \times 23)/(2 \times 173)$	C	$2773/2781 = (47 \times 59)/(3^3 \times 103)$

The reciprocal value of the ratio $(T_S - T_{SID})/T_{SID}$ which appears in Equation (7) determines the number of days in the solar or tropical year. Consequently, the clock mechanism produces an approximation of the mean tropical year of $T_T = 365.242189$ days [6] with an error whose absolute value can be determined by Equation (10).

$$\left| T_T - T_S \frac{\overline{T}_{SID}}{T_S - \overline{T}_{SID}} \right| = |365.242189 - 365.2422884| = 9.94 \times 10^{-5} \text{ days} \approx 8.6 \text{ s} \quad (10)$$

After all calculations and evaluations presented in this section, it can be concluded that the rational approximations of real ratios R_{MZ}, R_{SPh}, R_{MZ} and R_{SN} are not perfect, but are sufficiently good and practically applicable for the synthesis of the astronomical clock mechanism. The next section is dedicated to this task.

7. The Clock Gear Trains

In accordance with the presented astronomical data and their approximated ratios, the design of the astronomical clock mechanism is realized and a fully operational 3D model of this mechanical device is created by using the SolidWorks 2016 application (Dassault Systèmes, Dassault Group, Vélizy-Villacoublay, France).

As is shown in Figure 8, the mechanism of the clock consists of five gear trains. Each gear train had its specific speed ratio determined in the previous section by the method of continued fractions as the best rational and practically applicable approximation of the real ratios. The prime factors of the numerator and denominator of these approximated ratios are also calculated and the proper gear modulus and the number of teeth are determined. These ratios, the number of gear teeth and gear modulus are given in Table 6. The problem of selecting the best but practically applicable convergents or semi-convergents of the continued fraction approximation for the construction of the clock gears must be emphasized again. Obviously, higher terms of this rational approximation produce smaller errors. However, the higher terms have larger numerators and denominators and, very often, their prime factors are also huge. Since these prime factors have to be realized directly and precisely by the number of gear teeth, extremely high terms of continued fraction approximations are not practical and useful. On the other hand, lower terms of rational approximation are usable but produce larger errors. Thus, the problem of selecting the best but practically applicable convergents or semi-convergents of the continued fraction approximation must be solved as a compromise between two opposite demands.

The mechanism of the astronomical clock has four coaxial shafts which hold the lunar nodes, the Sun, the zodiac and the Moon pointers. Additionally, the clock mechanism is equipped with one separate shaft which controls the rotation of the sphere, which is painted

half white and half dark blue and displays the lunar phase. As was already emphasized and shown in the operational scheme of the clock mechanism in Figure 8, the shafts are mutually connected by five previously mentioned gear trains. The clock mechanism has two five-pointed frames which support the astronomical face, with all shafts and gear trains as one functional block.

Table 6. The rational approximations of the gear train ratios of the clock mechanism.

Ratio between the Pointers' Angular Velocities	Approximated Ratio	Approximated Ratio Indicated by the Number of Gear Teeth	Modulus (mm)
of the input clock hour pointer and the Sun R_{CS}	$\frac{2}{1}$	$\frac{40}{60} \times \frac{60}{80}$	2
of the Sun and the lunar phases R_{SPh}	$\frac{945}{32} = \frac{3^3 \times 5 \times 7}{2^5}$	$\frac{50}{20} \times \frac{50}{20} \times \frac{45}{20} \times \frac{42}{20}$	2
of the Sun and the Moon R_{SM}	$\frac{945}{913} = \frac{3^3 \times 5 \times 7}{11 \times 83}$	$\frac{70}{83} \times \frac{81}{66}$	1.5–70, 83 1.56122–81, 66
of the Moon and the Zodiac R_{MZ}	$\frac{26,001}{26,986} = \frac{3^5 \times 107}{2 \times 103 \times 131}$	$\frac{60}{131} \times \frac{81}{103} \times \frac{90}{60} \times \frac{107}{60}$	1
of the Sun and lunar nodes R_{SN}	$\frac{2773}{2781} = \frac{47 \times 59}{3^3 \times 103}$	$\frac{59 \times 94}{103 \times 54}$	1.5–59, 103 1.64189–94, 54

The gear trains which control the motion of the Sun pointer and the lunar phase's spherical display are shown in Figure 9 and the related gear numbers are given in Table 6. The gear modules for both trains are 2 mm. The Sun gear train consists of three gears, the first of which is connected to the hour shaft of the ordinary clock. This shaft holds the Sun pointer equipped with a small gold-plated symbol of the Sun. The hour shaft of this clock drives all gear trains of the astronomical clock. The lunar phase train has four pairs of gears and takes the power from the Sun shaft. The last shaft of the lunar phase's gear train is connected to the small spherical pointer which displays the current Moon phase.

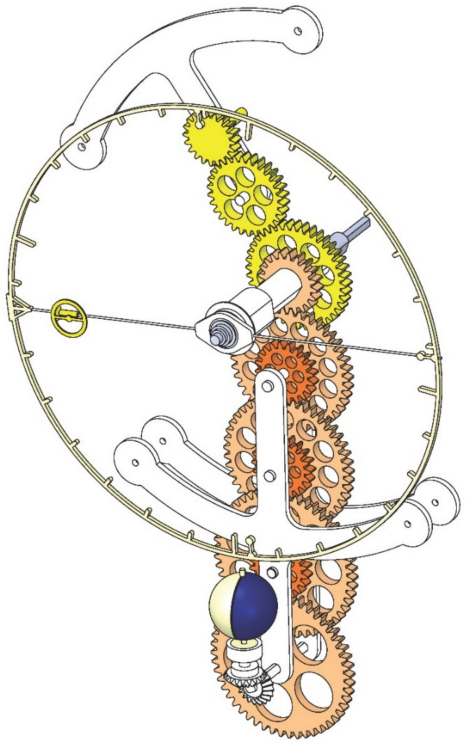

Figure 9. The Sun and the lunar phase gear trains.

The Moon gear train is shown in Figure 10. It consists of two pairs of gears, the first of which has a 2 mm modulus and the module of the second pair (1.56122 mm) is adjusted in such a way that the shafts of the first and the last gear are coaxial. The first gear of the Moon gear train is driven by the Sun shaft and the last gear drives the Moon pointer equipped with a small silver-plated symbol of the Moon. The numbers of teeth for each gear in the Moon gear train are given in Table 6. The support for this train is connected to the main pair of the astronomical clock's five-pointed frames.

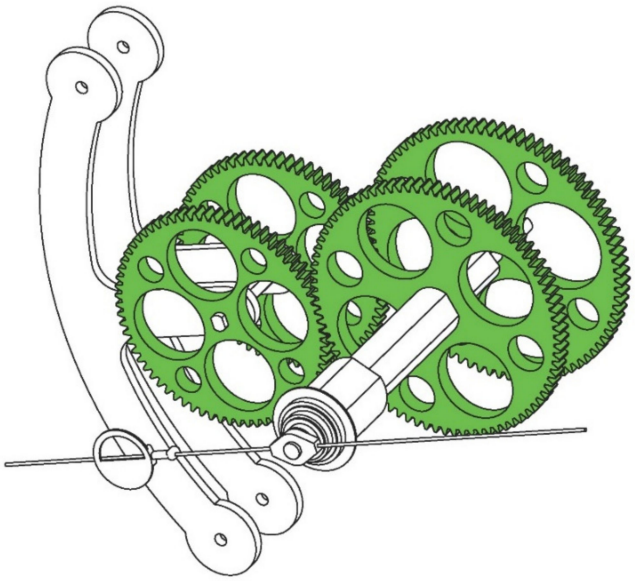

Figure 10. The Moon gear train.

The zodiac gear train is shown in Figure 11. It consists of four pairs of gears whose modulus is 1 mm. The number of teeth for each gear of this gear train is also given in Table 6. The first gear of the zodiac train is driven by the Moon shaft and the last gear drives the zodiac shaft to which the zodiac circle is attached. As was previously mentioned, the zodiac circle is divided into twelve equal segments which are equally graduated with six divisions of five degrees each. It measures the ecliptic longitudes of the Sun, the Moon and the lunar nodes.

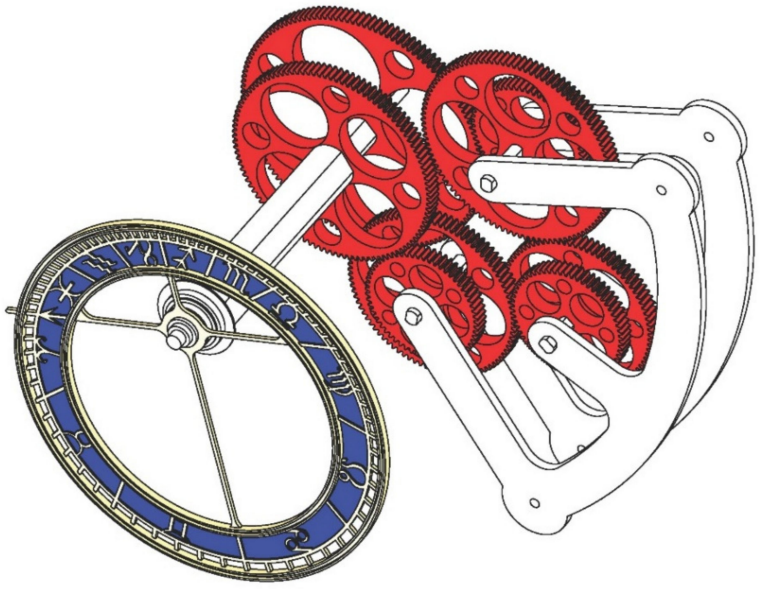

Figure 11. The zodiac gear train.

The lunar node gear train is shown in Figure 12. It consists of two pairs of gears, the first of which has a 1.5 mm modulus and the modulus of the second pair (1.64189 mm) is adjusted in such a way that the shafts of the first and the last gear are coaxial. As is done for the other gears, the numbers of teeth of the lunar node gear train are given in Table 6. The first gear of the lunar node train is driven by the Sun shaft and the last gear drives the lunar node pointer, shown in Figure 13. This pointer is equipped with two circular sectors which have ±9°30′ ±12°15′ ±15°23′ and ±18°35′ marks, the meaning of which was explained earlier. The angular span of this circular sector corresponds to a certain interval of time called the eclipse season during which the conditions for the occurrence of a solar or lunar eclipse are satisfied.

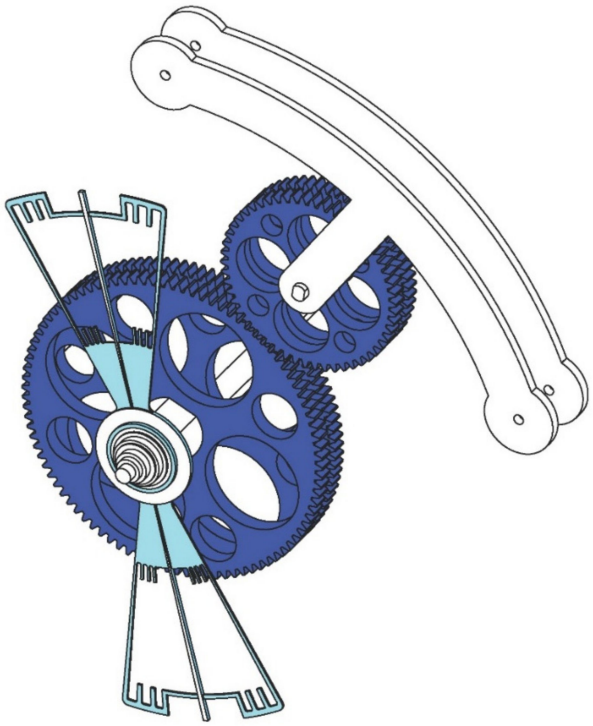

Figure 12. The lunar node gear train.

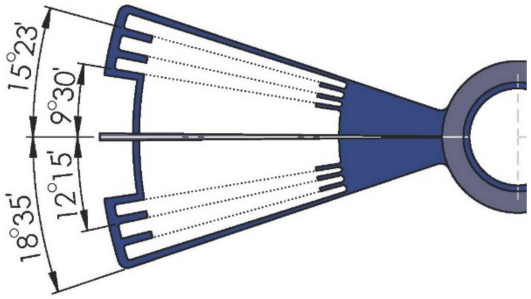

Figure 13. The lunar node and eclipse sector.

Figure 14 shows the complete assembly of the astronomical clock mechanism with the position of all gears. In this figure, 1 is the input shaft driven by the hour arbor of the ordinary clock, 2—the Sun gear train, 3—the Moon gear train, 4—the lunar phase train, 5—the main shaft of the astronomical clock, 6—the zodiac gear train, 7—the clock five-pointed frame and 8—the lunar node train.

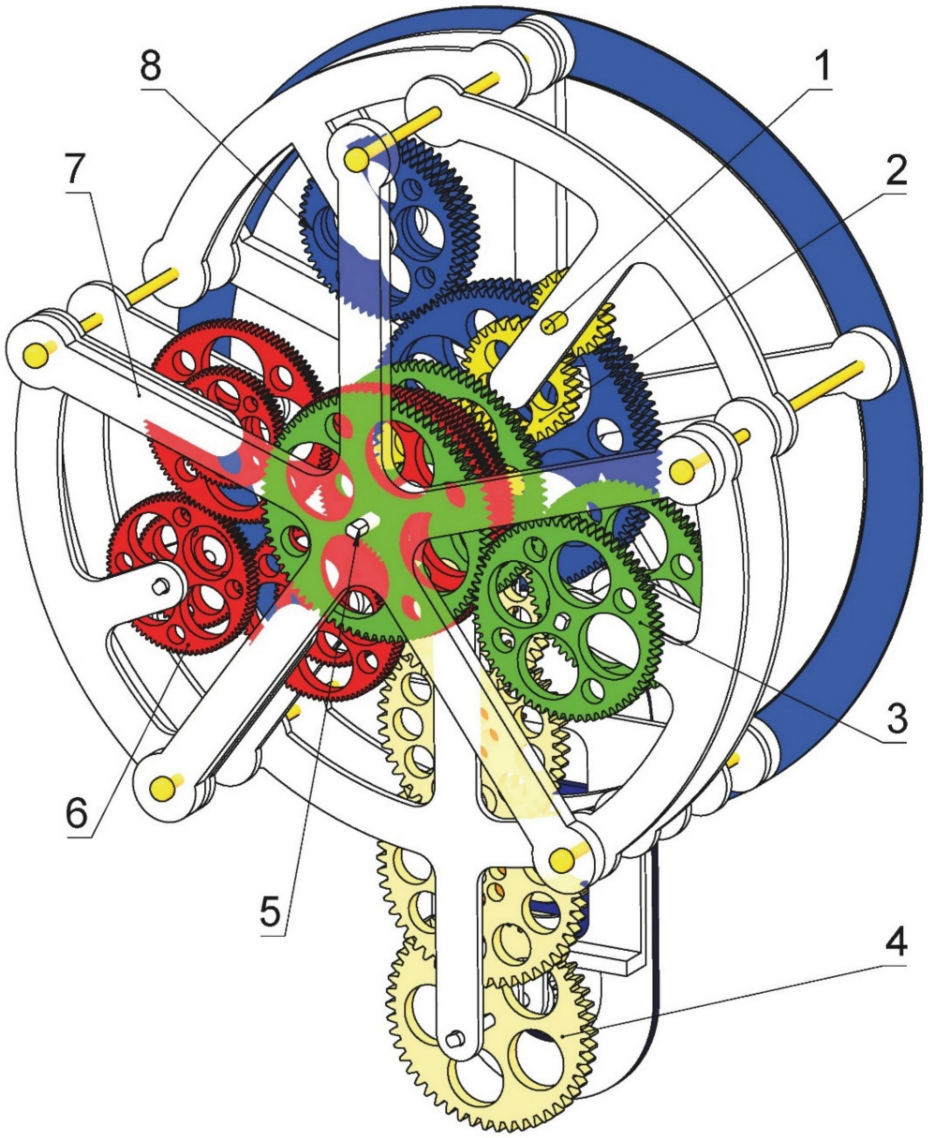

Figure 14. The assembly of the astronomical clock mechanism.

8. The Set-Up of the Clock Mechanism Motion Study

For the correct operation of the astronomical clock mechanism, the initial positions of the Sun, the Moon, the zodiac, the lunar phase and the lunar node pointers must be chosen first. The best way to accomplish this task is to adjust the pointers' positions for the date on which the Moon is located in its orbital perigee or apogee. This decision is reasonable since the modeled clock mechanism exclusively determines the mean motions and positions of the aforementioned astronomical objects and the true and mean position of the Moon in its orbital apogee or perigee is approximately the same. The Moon was in apogee on 18 May 2020 [14] and this date has been chosen for the astronomical clock set-up. The ecliptic longitudes for the Sun, the Moon and the lunar node ☊ are taken from ephemeris tables for 2020 [15] which are calculated for each day at Greenwich Mean Midnight. On 18 May 2020 at midnight 00:00 UT, the ecliptic longitude of the Sun was ☌ 27.52°, that of the Moon ☽ 5.13° and the mean longitude of the lunar node ☊ was S 0.93°. If the clock is located in Belgrade, latitude 20°28′, it is necessary to calculate the local mean solar time for this place. This is done by the following calculation [16]:

$$LSoT = LST + 4'(LL - LSTM) + ET = 1 + 4'(20.467 - 15) + 0 = 1:21:52 \quad (11)$$

In Equation (11), *LSoT* is the local solar time, *LST* the local standard time, *LL* the local longitude, *LSTM* the local standard time meridian measured in degrees which runs through the center of each time zone and *ET* is the equation of time. Neglecting *ET*, the local solar time becomes local mean solar time. In accordance with these data, the initial positions of the Sun, the Moon, the zodiac, and the lunar node pointers are adjusted on the astronomical clock face. The correct lunar phase is determined by the angular distance between the Sun and the Moon pointers.

After the clock pointers have been adjusted, the parameters of the mechanism motion study are also determined. A rotary motor with an angular velocity of 30 rpm is attached to the clock input shaft and the kinematic simulation is performed with 36 steps per second.

9. Results of the Clock Mechanism Motion Study

The motion study of this mechanism is accomplished by the use of the SolidWorks 2016 application and the accuracy of its predictions is demonstrated, documented and inspected. The simulation of the mechanism operation was performed continuously for 44 days, from 18 May to 30 June 2020. This particular period of 44 days was chosen because it contains all the astronomical events important for the initialization and the inspection of the clock operation. The longer simulation period will not reveal any essentially new characteristics of the clock performances. Since the Sun pointer of the clock model accomplishes one complete rotation in 4 s, 44 days take 176 s of simulation. The results of the clock mechanism motion study were obtained by measuring the angular coordinates of the corresponding pointers automatically every 4 s. All angular coordinates and the differences between the ephemeris astronomical data and the data generated by the motion study of the astronomical clock mechanism are collected and disclosed in Table 7. Columns A-*Eph*, K-*Eph* and N-*Eph* show ecliptic longitude for the Sun, the Moon and the lunar node, respectively, taken from ephemeris data. Columns A-*S*, K-*S* and N-*S* show the corresponding ecliptic longitudes obtained by the clock mechanism motion study and columns Δ A, Δ K and Δ N show the differences between them.

Table 7. Differences between ephemeris astronomical data and data generated by the motion study of the astronomical clock mechanism in angular degrees.

Date	A-*Eph*	A-*S*	ΔA	K-*Eph*	K-*S*	ΔK	N-*Eph*	N-*S*	ΔN
18.5	♌ 27.52	♌ 27.52	0	♍ 5.13	♍ 5.13	0	♋ 0.93	♋ 0.93	0
19.5	♌ 28.48	♌ 28.51	+0.03	♍ 17.00	♍ 18.31	+1.31	♋ 0.88	♋ 0.88	0
20.5	♌ 29.44	♌ 29.49	+0.05	♍ 28.92	♌ 1.48	+2.56	♋ 0.83	♋ 0.83	0
21.5	♎ 0.41	♌ 0.48	+0.07	♌ 10.92	♌ 14.66	+3.74	♋ 0.77	♋ 0.77	0
22.5	♎ 1.37	♌ 1.46	+0.09	♌ 23.07	♌ 27.83	+4.76	♋ 0.72	♋ 0.72	0
23.5	♎ 2.33	♌ 2.45	+0.12	♎ 5.35	♎ 11.01	+5.66	♋ 0.67	♋ 0.67	0
24.5	♎ 3.29	♌ 3.44	+0.15	♎ 17.80	♎ 24.19	+6.39	♋ 0.62	♋ 0.62	0
25.5	♎ 4.25	♎ 4.42	+0.17	♋ 0.45	♋ 7.36	+6.91	♋ 0.57	♋ 0.56	+0.01
26.5	♎ 5.22	♎ 5.41	+0.19	♋ 13.30	♋ 20.54	+7.24	♋ 0.50	♋ 0.51	+0.01
27.5	♎ 6.18	♎ 6.39	+0.21	♋ 26.38	♌ 3.71	+7.33	♋ 0.45	♋ 0.46	+0.01
28.5	♎ 7.14	♎ 7.38	+0.24	♌ 9.72	♌ 16.89	+7.17	♋ 0.40	♋ 0.40	0
29.5	♎ 8.09	♎ 8.37	+0.28	♌ 23.30	♍ 0.06	+6.76	♋ 0.35	♋ 0.35	0
30.5	♎ 9,05	♎ 9.35	+0.30	♍ 7.15	♍ 13.24	+6.09	♋ 0.30	♋ 0.30	0
31.5	♎ 10.01	♎ 10.34	+0.33	♍ 21.27	♍ 26.41	+5.14	♋ 0.25	♋ 0.24	−0.01
1.6	♎ 10.97	♎ 11.32	+0.35	♎ 5.63	♎ 9.59	+3.96	♋ 0.18	♋ 0.19	+0.01
2.6	♎ 11.93	♎ 12.30	+0.37	♎ 20.18	♎ 22.77	+2.59	♋ 0.13	♋ 0.14	+0.01
3.6	♎ 12.89	♎ 13.29	+0.40	♏ 4.83	♏ 5.95	+1.12	♋ 0.08	♋ 0.08	0
4.6	♎ 13.84	♎ 14.28	+0.44	♏ 19.50	♏ 19.17	−0.33	♋ 0.03	♋ 0.03	0
5.6	♎ 14.82	♎ 15.27	+0.45	♐ 4.07	♐ 2.30	−1.77	♎ 29.98	♎ 29.98	0
6.6	♎ 15.76	♎ 16.24	+0.48	♐ 18.42	♐ 15.48	−2.94	♎ 29.93	♎ 29.93	0
7.6	♎ 16.72	♎ 17.24	+0.52	♑ 2.47	♐ 28.65	−3.82	♎ 29.87	♎ 29.87	0

Table 7. *Cont.*

Date	A-*Eph*	A-*S*	ΔA	K-*Eph*	K-*S*	ΔK	N-*Eph*	N-*S*	ΔN
8.6	♑ 17.67	♑ 18.22	+0.55	♑ 16.18	♑ 11.83	− 4.35	♑ 29.82	♑ 29.82	0
9.6	♑ 18.63	♑ 19.21	+0.58	♑ 29.50	♑ 25.00	− 4.5	♑ 29.77	♑ 29.77	0
10.6	♑ 19.58	♑ 20.19	+0.61	♒ 12.47	♒ 8.18	−4.29	♑ 29.72	♑ 29.71	−0.01
11.6	♑ 20.54	♑ 21.18	+0.64	♒ 25.08	♒ 21.36	−3.72	♑ 29.67	♑ 29.67	0
12.6	♑ 21.49	♑ 22.16	+0.67	♓ 7.40	♓ 4.53	−2.87	♑ 29.60	♑ 29.61	+0.01
13.6	♑ 22.01	♑ 23.15	+1.14	♓ 19.50	♓ 17.71	−0.79	♑ 29.55	♑ 29.55	0
14.6	♑ 23.41	♑ 24.14	+0.73	♈ 1.47	♈ 0.89	−0.58	♑ 29.50	♑ 29.50	0
15.6	♑ 24.36	♑ 25.12	+0.76	♈ 13.35	♈ 14.06	+0.71	♑ 29.45	♑ 29.45	0
16.6	♑ 25.32	♑ 26.11	+0.79	♈ 25.23	♈ 27.24	+2.01	♑ 29.40	♑ 29.40	0
17.6	♑ 26.27	♑ 27.01	+0.74	♉ 7.18	♉ 10.41	+3.23	♑ 29.35	♑ 29.34	+0.01
18.6	♑ 27.23	♑ 28.08	+0.85	♉ 19.28	♉ 23.59	+4.31	♑ 29.28	♑ 29.29	+0.01
19.6	♑ 28.18	♑ 29.06	+0.88	♊ 1.55	♊ 6.77	+5.22	♑ 29.23	♑ 29.24	+0.01
20.6	♑ 29.14	♒ 0.05	+0.91	♊ 14.03	♊ 19.94	+5.91	♑ 29.18	♑ 29.18	0
21.6	♒ 0.09	♒ 1.04	+0.95	♊ 26.77	♋ 3.12	+6.35	♑ 29.13	♑ 29.13	0
22.6	♒ 1.05	♒ 2.02	+0.97	♋ 9.75	♋ 16.29	+6.54	♑ 29.08	♑ 29.08	0
23.6	♒ 2.00	♒ 3.00	+1.00	♋ 22.98	♋ 29.47	+6.49	♑ 29.03	♑ 29.03	0
24.6	♒ 2.95	♒ 3.99	+1.04	♌ 6.45	♌ 12.65	+6.20	♑ 28.97	♑ 28.97	0
25.6	♒ 3.91	♒ 4.98	+1.07	♌ 20.13	♌ 25.82	+5.69	♑ 28.92	♑ 28.92	0
26.6	♒ 4.86	♒ 5.96	+1.10	♍ 4.02	♍ 9.00	+4.98	♑ 28.87	♑ 28.87	0
27.6	♒ 5.82	♒ 6.95	+1.13	♍ 18.05	♍ 22.17	+4.12	♑ 28.82	♑ 28.82	0
28.6	♒ 6.77	♒ 7.93	+1.16	♎ 2.20	♎ 5.35	+3.15	♑ 28.77	♑ 28.76	−0.01
29.6	♒ 7.72	♒ 8.92	+1.20	♎ 16.43	♎ 18.53	+2.10	♑ 28.70	♑ 28.71	+0.01
30.6.	♒ 8.68	♒ 9.91	+1.23	♏ 0.72	♏ 1.70	+0.98	♑ 28.65	♑ 28.66	+0.01

10. Discussion

Analyzing the data collected in Table 7 and regarding the features of the modeled astronomical clock, the following remarks and conclusions can be drawn:

1. Throughout the duration of 44 days, the differences for the Sun longitudes between the ephemeris data and the data obtained by the motion study of the clock mechanism operation gradually grow from 0° to +1.23°. This divergence occurs because the clock mechanism neglects the equation of time and tracks only the mean motion of the Sun. This error induces the difference between the true and the mean local time.
2. During the 44 days, the differences for the Moon longitudes between the ephemeris data and the data obtained by the simulation have positive and negative signs and their absolute values are larger than those calculated for the Sun. These errors are expected since the orbit and the motion of the Moon have many irregularities and the Moon gear train of the clock mechanism displays only its uniform motion and determines its mean positions. Moreover, since the clock is adjusted for the date on which the Moon is located in its orbital apogee, the Moon mean positions obtained by the simulation "oscillate" around the correct positions on both sides, between −4.36° and +7.35°.
3. The mean longitudes of the lunar node N determined by the mechanism motion study are identical to those given in ephemeris tables. This means that the lunar nodes gear train generates good approximation for the mean precession of the lunar nodes.
4. During June 2020, two significant and interesting astronomical events occurred, the first of which was the lunar eclipse and the second one was the solar eclipse. The eclipse of the Moon was penumbral and took place on 5–6 June 2020 [17] and the solar eclipse was annular and occurred on 21 June 2020 [18]. Since it is equipped with the lunar node pointer, the astronomical clock presented in this work was able to predict these events with acceptable accuracy. In Belgrade, the lunar eclipse began on 5 June at 19:45:51 CET, reached its maximum at 21:24:55 CET and ended at 23:04:03 CET. The astronomical clock predicted the beginning of the lunar eclipse on 5 June

2020 at approximately 16:42 when the Moon pointer entered the eclipse sector and the maximum at 23:16 when the Moon pointer overlapped the Sun pointer inside the eclipse sector, as is shown on Figure 15. (The clock tells local mean solar time for Belgrade.) The end of the eclipse could not be determined by the positions of the Sun, the Moon and the lunar node pointers of the clock. The error of the clock prediction was visible but it was not too large. In Belgrade, the annular solar eclipse reached its maximum on 21 June 2020 at 8:40:04 CET and, as is shown in Figure 16, the astronomical clock predicted that this maximum would occur on 20 June 2020 at 17:58 when the Moon icon overlapped the Sun icon inside the eclipse sector and almost overlapped the nodal pointer. The error was quite large, more than 12 h ahead, but this was expected since the error range for the Moon longitude was also large (−4.36°, +7.35°). Predictions of the lunar and solar eclipses with similar values of error are obtained by an entirely different mechanical device described and explained in [19].

Figure 15. Full Moon and penumbral lunar eclipse of 5–6 June 2020.

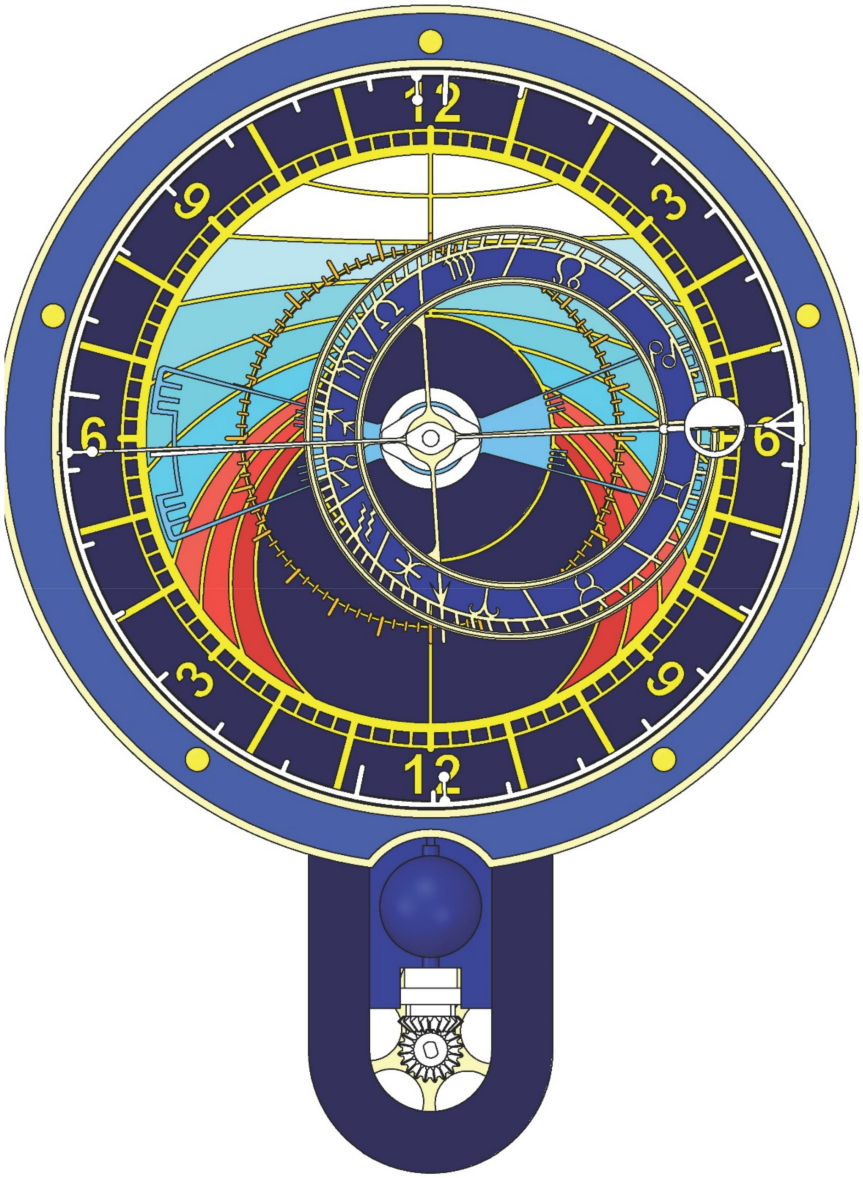

Figure 16. New Moon and annular solar eclipse of 21 June 2020.

It will be interesting to compare the design of the astronomical clock presented in this paper with the design of the famous Prague astronomical clock. Both clocks have similar dials, designed as the stereographic projection of the celestial sphere, and both of them display the motions and the mean positions of the Sun, Moon, zodiac circle and the Moon phases. As for the difference, the presented clock has the lunar node pointer which enables the prediction of lunar and solar eclipses. Moreover, this clock displays lunar phases in a more vivid way on a separate dial equipped with a rotational sphere which is painted half white and half dark blue. It is also significant to compare the accuracy of this clock with the accuracy of the Prague astronomical clock. The main mechanism of the Prague clock consists of three gears: one for the movement of the zodiac (365 teeth), one for the Sun (366 teeth) and one for the Moon (379 teeth) [20]. Regarding these facts, the Prague astronomical clock approximates the sidereal day as 23.93442623 h and tidal lunar day as 24.852459 h. The lunar phase mechanism has 59 gears and rotates by advancing two teeth per day [20]. Thus, this mechanism approximates the synodic month as 29.5 days. All three approximations are less accurate than equivalent approximations obtained by the astronomical clock whose design is presented in this paper. Thus, in comparison with the designed clock, the Prague astronomical clock has a much simpler mechanism

and consequently produces less accurate approximations of the motions and positions of celestial objects.

11. Final Remarks and Conclusions

This work presents the design of an astronomical clock which displays the mean position of the Sun, the Moon, the lunar nodes and the zodiac circle and their motions during the year geocentrically. Since the mean periods of motions are approximated by the method of continued fractions and realized by a set of gear trains with great accuracy, the clock mechanism determines the mean positions of the aforementioned astronomical object correctly. Nevertheless, the accuracy of the presented astronomical clock can be improved by a more advanced and delicate mechanism which considers non-uniform motions of the Moon and the Earth. For this purpose, the paper [21] is of great interest, since it shows the kinematic structure of Dondi's astronomical clock, whose gear trains are equipped with non-circular gears for tracking the motion of the Moon and the planet Mercury. For similar reasons, the paper [22] is also interesting since it presents a concept of an epicyclical gear train able to generate a variable gear ratio law. The authors of this paper have already examined and prepared several epicyclical mechanisms that take into account the equation of time as well as the first and the second lunar anomalies. By the use of these mechanical devices, the novel astronomical clock will be capable of simulating and displaying the visible motions of the Earth and the Moon more accurately.

It must be emphasized again that the astronomical dial of this clock is constructed for the latitude of Belgrade (44.8° N). Since the stereographic projection of the celestial sphere is altered only by a change of latitude, this clock can be installed in any place on the Earth with the latitude 44.8° N. For places with different latitudes, the clock mechanism stays unchanged and only the astronomical dial should be adjusted by the principles given in this work.

This paper could be important, mostly for education in the field of mathematics, geometry, the theory of mechanisms, 3D modeling and motion study, as well as for teaching courses in astronomy. Moreover, the presented methods of the clock mechanism synthesis can be useful for the design, maintenance and conservation of large-scale city astronomical clocks since these clocks represent a precious historical and cultural heritage of European civilization. The main contribution of this work lies in disseminating and protecting knowledge, the loss of which risks making these precious clocks no longer restorable.

Author Contributions: Conceptualization, B.P. and Z.M.; Methodology, B.P. and M.S.; Validation, Z.M.; Formal analysis, I.C. and I.V.; Investigation, B.P. and R.O.; Resources, M.S., Z.J. and Z.M.; Software, B.P., M.S. and Z.J.; Writing—original draft preparation, B.P., R.O., M.S. and I.C.; Writing—review and editing, R.O. and I.C., Visualization, B.P., R.O., M.S., Z.J. and I.V.; Supervision, B.P. and R.O.; Project administration, R.O.; Funding acquisition, B.P. and R.O. All authors have read and agreed to the published version of the manuscript.

Funding: This research received no external funding.

Institutional Review Board Statement: Not applicable.

Informed Consent Statement: Not applicable.

Data Availability Statement: Not applicable.

Acknowledgments: This research is supported by the Ministry of Science and Education of the Republic of Serbia, Grant 451-03-9/2021-14/200105 05.02.2021.

Conflicts of Interest: The authors declare no conflict of interest.

References

1. Cvetković, I.; Popkonstantinović, B.; Stojićević, M.; Obradović, R.; Milicević, R. Stereographic projection of the heavens over belgrade used for the construction of astronomical city clock. *J. Ind. Des. Eng. Graph.* **2019**, *14*, 57–60.
2. "Le Gros-Horloge", Photo by Daniel Vorndran/DXR. Available online: http://rouen-histoire.com/GHorloge/index.htm (accessed on 1 April 2021).

3. Strasburg Clock. Available online: https://commons.wikimedia.org/wiki/File:Strasbourg_Cathedral_Astronomical_Clock_-_Diliff.jpg (accessed on 1 April 2021).
4. Prague Astronomical Clock. Available online: https://commons.wikimedia.org/wiki/File:Astronomical_Clock_(8341899828).jpg (accessed on 1 April 2021).
5. Slovenský Orloj v Starej Bystrici. Available online: https://en.wikipedia.org/wiki/Star%C3%A1_Bystrica#/media/File:Star%C3%A1_Bystrica1.jpg (accessed on 1 April 2021).
6. Reingold, M.E.; Dershowitz, N. *Calendrical Calculations: The Ultimate Edition*, 4th ed.; Cambridge University Press: Cambridge, UK, 2018.
7. *Astronomical Almanac for the Year 2019*, Annual ed. (4 January 2018); Department of the Navy: Monterey, CA, USA, 2018.
8. Van den Bergh, G. *Periodicity and Variation of Solar (and Lunar) Eclipses*; Tjeenk Willink & Zn NV: Haarlem, The Netherlands, 1955; Volume 2.
9. Ryan, J. *Eclipses Illustrated: Book 2—Eclipses and the Orbit of the Moon: A Visual Approach to Understanding Eclipses of the Sun and Moon*, Kindle ed.; American Eclipse USA, 2017.
10. Mitton, S. *The Cambridge Encyclopaedia of Astronomy Hardcover—1 January 1977*, 1st ed.; Crown: New York, NY, USA, 1977.
11. Khinchin, Y.A. *Continued Fractions*; University of Chicago: Chicago, IL, USA, 1964.
12. Milinkovic, L.; Malesevic, B.; Banjac, B. Continued fractions, intermediate fractions and their relation to the best approximations. *J. Sci. Arts* **2020**, *20*, 545–560. [CrossRef]
13. Malešević, B.; Milinković, L. *Verižni Razlomci i Primene, Simpozijum MATEMATIKA I PRIMENE, Matematički Fakultet*; Univerzitet u Beogradu: Belgrade, Serbia, 2014; Volume V(1).
14. *Lunar Tables and Programs from 4000, B.C. to A.D. 8000*, 1st ed.; Willmann-Bell: Richmond, VA, USA, 1991.
15. *Raphael's Astronomical Ephemeris of the Planets' Places for 2020*; Foulsham & Co., Ltd.: Harrow, UK, 2019.
16. Abdurrahman, M.; Gambo, J.; Shitu, I.G.; Yusuf, Y.A.; Dahiru, Z.; Idris, A.M.; Isah, A.A. Solar elevation angle and solar culmination determination using celestial observation; a case study of hadejia jigawa state, Nigeria. *Int. J. Adv. Sci. Res. Eng.* **2019**, *5*, 301–308. [CrossRef]
17. Five Millennium Catalog of Solar Eclipses: −1999 to +3000 (2000 BCE to 3000 CE). Available online: https://eclipse.gsfc.nasa.gov/5MCLE/5MKLE-214173.pdf (accessed on 1 April 2021).
18. Five Millennium Catalog of Solar Eclipses: −1999 to +3000 (2000 BCE to 3000 CE). Available online: https://eclipse.gsfc.nasa.gov/5MCSE/TP2009-214174.pdf (accessed on 1 April 2021).
19. Popkonstantinović, B.; Miladinović, L.; Obradović, R.; Jeli, Z.; Stojićević, M. The Eclipses Abacus, the mechanical predictor of the solar and lunar eclipses. *SAGE J. Simul.* **2018**. [CrossRef]
20. The Prague Astronomical Clock. Available online: http://www.orloj.eu/en/orloj_kovarske.htm (accessed on 1 April 2021).
21. Addomine, M.; Figliolini, G.; Pennestri, E. *A Landmark in the History of Non-Circular Gears Design: The Mechanical Masterpiece of Dondi's Astrarium, Mechanism and Machine Theory*; Elsevier: Amsterdam, The Netherlands, 2018; Volume 122, pp. 219–232. [CrossRef]
22. Mundo, D. *Geometric Design of a Planetary Gear Train with Non-Circular Gears, Mechanism and Machine Theory*; Elsevier: Amsterdam, The Netherlands, 2006; Volume 41, pp. 456–472. [CrossRef]